



## ANALYSIS OF GUIDED WAVE PROPAGATION IN ADHESIVE JOINTS OF STEEL RODS

Erwin WOJTCZAK, Magdalena RUCKA

Gdańsk University of Technology, Faculty of Civil and Environmental Engineering,  
Department of Mechanics of Materials and Structures, Narutowicza 11/12, 80-233 Gdańsk, Poland  
e-mail: [erwin.wojtczak@pg.edu.pl](mailto:erwin.wojtczak@pg.edu.pl), [magdalena.rucka@pg.edu.pl](mailto:magdalena.rucka@pg.edu.pl)

### Abstract

The aim of the study is the elastic wave propagation in adhesive joints of metal rods that are one of the simplest kind of glue connections. They are consisted of two metal members and an adhesive layer joining two parts together. The analysis is directed to technical diagnostics of such type of connections. Longitudinal and transversal guided waves were excited in prepared joints. Signals of propagating waves were registered in a couple of points by means of PZT plate sensors. Butt and single lap joints were tested. Single rod was also investigated to compare with adhesive joints. There were two approaches applied for both types of connections: experimental investigations and FEM analysis. In the study, the possibility of the application of guided waves in diagnostics of adhesive joints of metal rods was analysed.

Keywords: guided waves, adhesive joints, non-destructive testing, FEM

### ANALIZA PROPAGACJI FAL PROWADZONYCH W POŁĄCZENIACH KLEJONYCH PRĘTÓW STALOWYCH

#### Streszczenie

Tematem niniejszej pracy jest propagacja fal sprężystych w połączeniach klejonych prętów metalowych, które są jednymi z najprostszych typów złączy adhezyjnych. Składają się one z dwóch elementów stalowych oraz łączącej je spoiny klejowej. Analiza zjawiska została ukierunkowana na diagnostykę techniczną tego typu połączeń. W połączeniach wzbudzano fale prowadzone podłużne i poprzeczne. Sygnały propagującej fali zarejestrowano w kilku punktach rozmieszczonych na długości prętów za pomocą piezoaktuatorów płytkowych. Badaniom poddano połączenia doczołowe oraz zakładkowe pojedyncze. Pojedynczy pręt został przebadany celem porównania z połączeniami klejonymi. Dla obydwu rodzajów połączeń zastosowano dwa podejścia do problemu: pomiary eksperymentalne oraz analizę MES. W pracy przeanalizowano możliwości zastosowania fal prowadzonych w diagnostyce połączeń klejonych prętów metalowych.

Słowa kluczowe: fale prowadzone, połączenia klejone, badania nieniszczące, MES

## 1. INTRODUCTION

### 1.1. Characterization of adhesive joints

Adhesive joints are classified into a group of inseparable connections. Typically they are consisted of two or more adherends (technical term for joined elements) and adhesive film (glue layer). There exist many kinds of glue connections that are applicable in engineering structures [1]. Depending on intended use, the geometry of joints may differ significantly. The simplest and the most popular types of joints are: a butt joint (Fig. 1a) and a single lap adhesive joint (Fig. 1b). The connection is in general subjected to shearing or tension and its strength is determined by mechanical properties of applied glue and condition of surfaces of adherends in the area of overlay before combination. Designing of adhesive joints is not a trivial task. Any mistake committed during planning or constructing may result in a severe decrease of the load capacity of structural elements that is significant for the safety of engineering structures.



Fig. 1. Typical adhesive joints: a) butt joint, b) single lap joint

Structural adhesive joints are widely used in timber structures. For example glue laminated wood is willingly applied for long span girders in roof structures. Glue connections have also many applications for metal structures, e.g. in automotive and aerospace industry [1]. Aluminium parts of aircraft fuselage have been joined with the use of phenolic adhesives since 1940s [4]. Regarding civil engineering, adhesive joints were successfully applied in bridge structures. In 1950s in Germany a truss bridge was constructed with the use of epoxy adhesive [10]. In 1963 in Poland a compound footbridge was erected from steel I-beam girders and reinforced concrete slabs.

Nowadays, structural gluing is applied for constructing elevations of representative buildings, e.g. skyscrapers [5]. Another significant application is strengthening of existing structures or their elements, e.g. thickening of webs of steel plate girders or gluing an external reinforcement to concrete and masonry ceilings, beams, columns and walls [9, 12].

Adhesive joints have numerous advantages. One of the most significant issues is the possibility of creating heterogenic connections (between adherends of different materials). Another question is the lack of intrusion in the internal structure of bonded elements as it takes place in welded and bolted joints. On the other hand, there are some negative sides, like high vulnerability to dynamic impacts, thermal effects and inaccuracies in preparation process of the joint. A very troublesome question is a quality deterioration of adhesive layer in time [12]. These harmful effects are the trigger for rapid growth in the interest of non-destructive diagnostics and structural health monitoring systems [2, 13].

### 1.2. Guided waves in diagnostics

Mechanical wave is a disturbance travelling in an elastic medium and transporting energy through motion of particles [14]. If the medium is infinite, it exists as a bulk wave in the form of pressure or shear wave, one of two types that propagates independently. Real engineering structures are consisted of elements with finite dimensions providing boundaries that are essential for guided wave existence. For example, Lamb waves are specific kind of guided waves that occur in media restrained by two parallel surfaces like thin plates. In one-dimensional elements like rods, axial (longitudinal) and flexural waves exist. Both are dispersive, i.e. their characteristics are frequency-dependent. Diagrams representing this relations are so-called dispersion curves.

Diagnostic methods based on guided wave propagation have been dynamically developed over recent years [8, 13, 14]. They create a significant group of non-destructive testing techniques and became very efficient for inspection of existing structures, e.g. for damage detection. There are two essential approaches applied for exploration of adhesive joints. The first is the ultrasonic method (Fig. 2a), a local technique utilizing waves travelling through the thickness of the joint. It enables to receive a full profile of the adhesive layer but it also requires multiple measurements [7]. Another approach is guided wave propagation method (Fig. 2b) that gives effective results in one measurement. It was successfully applied for diagnostics of steel plates [14], bolted joints [6], ground anchors [15] and many more. Regarding adhesive connections, the wave is excited in one adherend, it propagates through the joint and then it is registered in another adherend. Collection of signals may happen simultaneously in a number of

points disposed on the whole structure. Proper interpretation of collected signals provides assessment of condition of the joint.

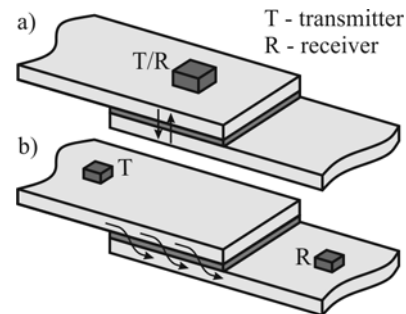


Fig. 2. Schemes of ultrasonic wave-based diagnostic techniques for inspection of adhesive joints: a) ultrasonic method, b) guided wave propagation method

## 2. OBJECT OF THE STUDY

The investigation was carried out on steel rods with square cross section of  $6 \times 6 \text{ mm}^2$ . Density and Young modulus of steel was acquired from measurements conducted on representative samples, obtaining  $7860 \text{ kg/m}^3$  and  $190 \text{ GPa}$ , respectively. Poisson ratio was assumed as 0.3 (mean value for steel). Mechanical parameters of applied metallic glue (POXIPOL) were taken from producer. Adhesive has a density  $1550 \text{ kg/m}^3$ , Young modulus  $3.43 \text{ GPa}$  and Poisson ratio 0.35. Measurements were carried out on different specimens: homogeneous rod (A, Fig. 3a), butt adhesive joint (B, Fig. 3b) and four types of single lap adhesive joints differing in length of overlay (C1-C4, Figs. 3c-f). Total length was constant for all specimens and equal to 960 mm.

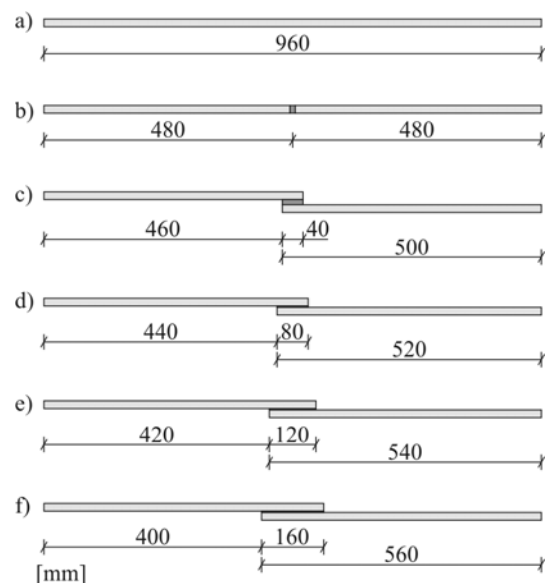


Fig. 3. Analysed rod specimens: a) homogeneous rod, b) butt joint, c)-f) single lap joints

### 3. FEM CALCULATIONS

Numerical analyses were conducted using Abaqus/Explicit software. Modelling of adhesive joint was simplified as possible. Isotropic homogeneous material model was assumed for steel and glue (with different mechanical parameters). Three-dimensional model was applied with the use of C3D8R elements (solid, cubic, 8-node elements with reduced integration). The general mesh size was 1 mm (adopted after [11]). Boundary conditions were free on all edges. The adhesive layer was modelled as an independent layer of elements attached rigidly to the surfaces of adherends. The excitation was a five-peak wave packet attained from sinusoidal function of 95 kHz frequency modulated by the Hanning window. The input signal in time and frequency domains is presented in Fig. 4. The obtained wave packet was used to excite the wave propagation in prepared models. Two excitation schemes were applied (Fig. 5). In the first one (L), a longitudinal wave was excited, whereas in the second scheme (F) flexural one was obtained. Dynamic/Explicit analysis was conducted for both schemes. The size of time step was assumed as  $10^{-7}$  s according to [11]. The explicit algorithm of the central difference method was used to solve the problem. The results of the analyses were acceleration maps for the whole model and acceleration values for selected nodes at the ends of the sample and spread over its length (Fig. 6).

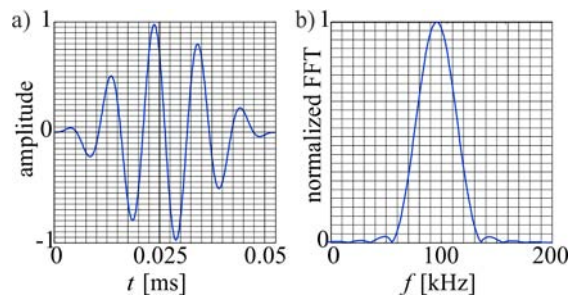


Fig. 4. Input wave signal: a) in time domain, b) in frequency domain

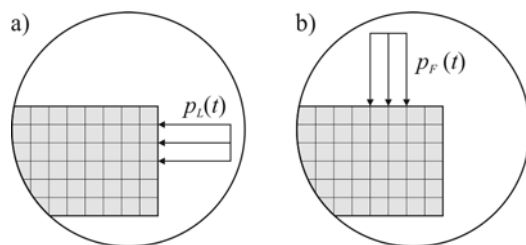


Fig. 5. Excitation schemes: a) longitudinal (L), b) flexural (F)

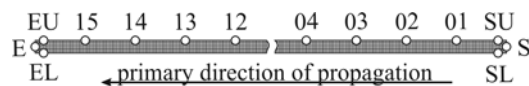


Fig. 6. Configuration of measurement points for exemplary of specimen A

### 4. EXPERIMENTAL MEASUREMENTS

Experimental models of specimens A, B and C1 were prepared from a single steel rod with a length of 3000 mm cut into appropriate pieces. The overlay area of each glued rod was treated before bonding with abrasive paper (type P120) and degreased with acetone. The thickness of adhesive layer was controlled with a vernier calliper to obtain approximately 1 mm. Prepared samples were retained in room temperature to gain a full guaranteed strength (24 hours).



Fig. 7. Experimental setup

Experimental setup is presented in Fig. 7. Guided waves were excited and sensed by plate PZT actuators Noliac NAC2011 with dimensions of  $2 \times 2 \times 2 \text{ mm}^3$ . Generation and acquisition of ultrasonic wave signals were provided by PAQ-16000D system. The excitation signal was assumed to be the same as implemented for numerical models. To obtain experimental results comparable with numerical ones, two excitation schemes were applied, namely inducing longitudinal and flexural waves. The outcome of measurements were time domain signals of propagating wave in certain points located at the ends of tested samples (Fig. 8).

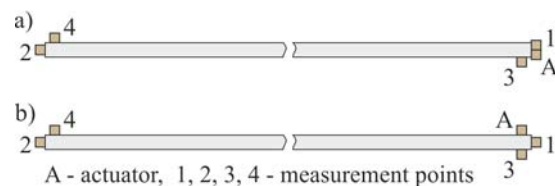


Fig. 8. Set of sensors for experimental measurements: a) scheme L, b) scheme F

To minimize random mistakes, each experimental specimen was examined five times and all the sensors were removed and attached again before each measurement. All data was analysed and representative signals were chosen for each specimen and scheme. Due to the delay of the input signal, beginnings of recorded signals were cut. To reduce environmental disturbances, a band-pass filter in a frequency range of 20-110 kHz was applied. The filter was prepared with the use of Butterworth polynomial approximation.

## 5. RESULTS

### 5.1. Homogeneous rod and butt adhesive joint

Figures 9a and 9b present acceleration maps in longitudinal and transversal directions for control sample A and scheme L, at particular time instances. It is clearly visible that two fundamental modes (symmetric S0 and antisymmetric A0) propagates in the rod with different velocities. The existence of A0 mode is possible because of non-ideal axial location of the excitation point. The symmetric mode occurrence collocates with higher values of axial acceleration whereas antisymmetric one is related to transverse acceleration.

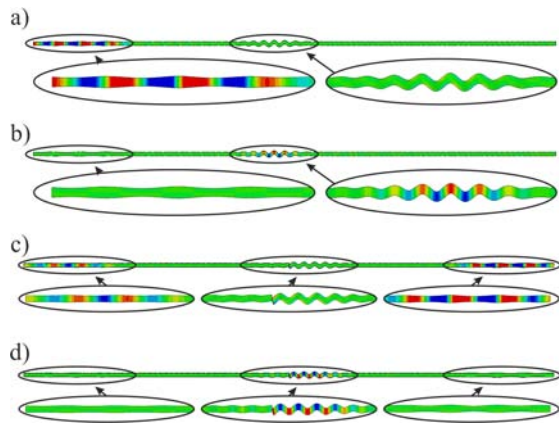


Fig. 9. Numerical acceleration maps (scheme L, time 0.2 ms): a) specimen A, axial direction, b) specimen A, transverse direction, c) specimen B, axial direction, d) specimen B, transverse direction

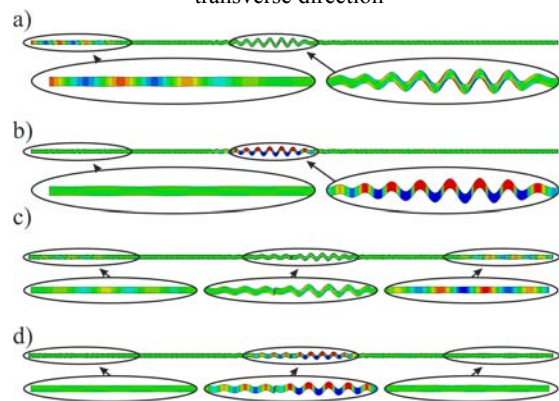


Fig. 10. Numerical acceleration maps (scheme F, time 0.2 ms): a) specimen A, axial direction, b) specimen A, transverse direction, c) specimen B, axial direction, d) specimen B, transverse direction

Figures 9c and 9d show analogical maps for specimen B. Likewise in homogeneous rod, S0 and A0 modes exist, but the wave propagation is disturbed by the butt joint in the middle of the bar. The joint may be treated as a defect; the wave modes are partially reflected and transmitted through it. For analysed time instance (0.2 ms) S0 mode occurs simultaneously at the end of the rod (transmitted part) and at the point of excitation

(reflected part). It can be observed that reflected wave transports much more energy than transmitted one. At the same time antisymmetric mode propagates through the joint. A disproportion between transmitted and reflected part is very clear. Similarly to specimen A, S0 mode is connected with axial acceleration, whereas A0 deals with transverse one. Observations from analysis of maps for samples A and B in scheme F at the same time instance (Fig. 10) are similar to these from scheme L. It is worth noticing that in scheme F mode S0 is hardly visible, only A0 is clearly observable whereas in scheme L both modes exist. The reason is the fact that excitation in scheme F has typically antisymmetric nature, whereas for scheme L it has both, symmetrical and antisymmetric features.

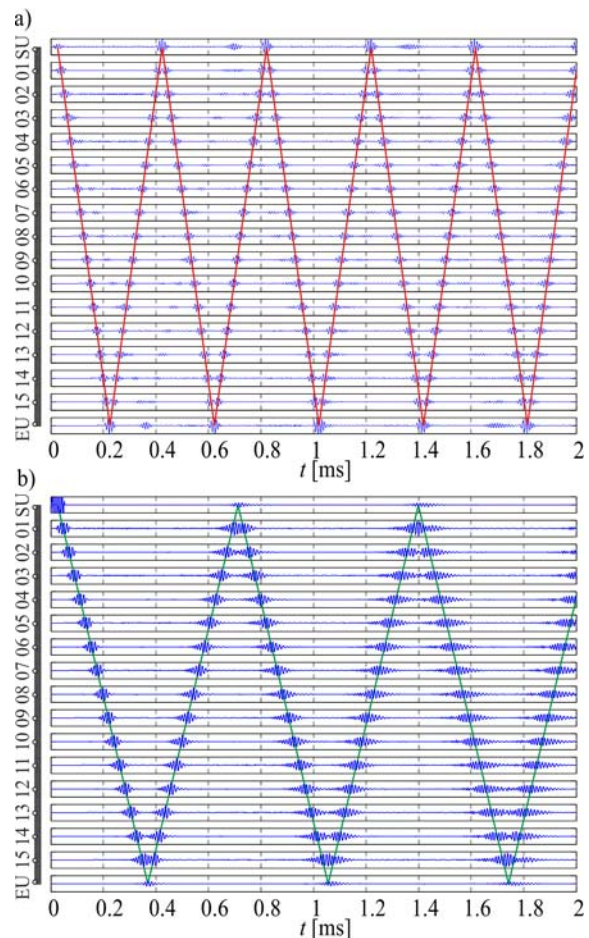


Fig. 11. Numerical signals for specimen A: a) scheme L, axial acceleration, b) scheme F, transverse acceleration

Figure 11 shows wave propagation signals collected at points spread over the length of specimen A in axial direction (scheme L) and in transverse direction (scheme F). Red lines link wave packets connected to S0 mode whereas the green ones join packets of A0 mode. The comparison of both charts gives a conclusion that symmetrical mode is strengthened when reflected at the end of the rod, but antisymmetric one is weakened. In scheme L, S0 and A0 modes are



visible (A0 is not marked to preserve the clarity of the chart) whereas only A0 is visible in scheme F.

The analysis of signals enabled to determine group velocity of both occurring modes. An interval between two wave packets in a starting point is a time that passes between two reflections, i.e. time when wave runs a distance of a double rod length. The identified group velocities for S0 and A0 modes, were 4857 m/s and 2797 m/s, respectively. Knowing that rod waves are dispersive, dispersion curves for the analysed bar were prepared (Fig. 12) with the use of *GUIGUW* software [3]. Calculated velocities for analysed frequency of 95 kHz for S0 and A0 modes were 2652 m/s and 4954 m/s, respectively.

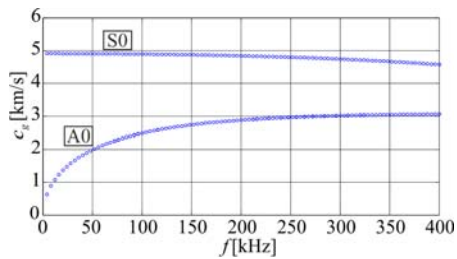


Fig. 12. Dispersion curves for steel rod with cross section of 6x6 mm<sup>2</sup>

Signals collected for butt joint sample are presented in Fig. 13. Propagation velocities of modes S0 and A0 are exactly the same as for homogeneous rod. A fundamental difference between specimens A and B is the existence of additional wave packets in signals for the butt adhesive joint that are marked by dashed lines. They represent reflections from the adhesive layer. Amplitudes of signals before and after passing through the joint indicate on disproportion between reflected and transmitted waves. What is interesting, a progressive transmission of propagating wave can be observed. With every following reflection amplitudes of signals before the joint were decreasing. Simultaneously, amplitudes of signals after the joint were increasing. When most of the wave energy was transmitted through the joint, the phenomenon became reversed. The effect occurred faster for S0 mode than for A0 mode.

Figures 14 and 15 presents wave propagation signals collected in experimental points 1 and 2 in schemes L and F for specimens A and B, respectively. Numerical signals are presented in the form of a Hilbert envelope (blue lines). The main difference between experimental and numerical results is a progressive decrease in amplitudes of measured signals. The reason of this effect is the attenuation that was not implemented in numerical models. For specimen A in scheme L there were wave packets of high amplitude (mode S0) and of lower amplitude (A0) but only in point 1 (Fig. 14a). In point 2 (Fig. 14b) antisymmetric mode was not visible, because the sensor was placed axially

whereas sensor 1 was located eccentrically. In scheme F, signals from points 1 and 2 reveal more disturbances (Figs. 14c and 14d), because these points are more sensitive for longitudinal waves. For specimen B (Fig. 15) there are extra wave packets responsible for reflections from the adhesive layer. Amplitudes of experimental and numerical signals differ significantly. The reason may be inaccuracy in mechanical parameters implemented to the model or a high degree of simplification in modelling of the adhesive layer.

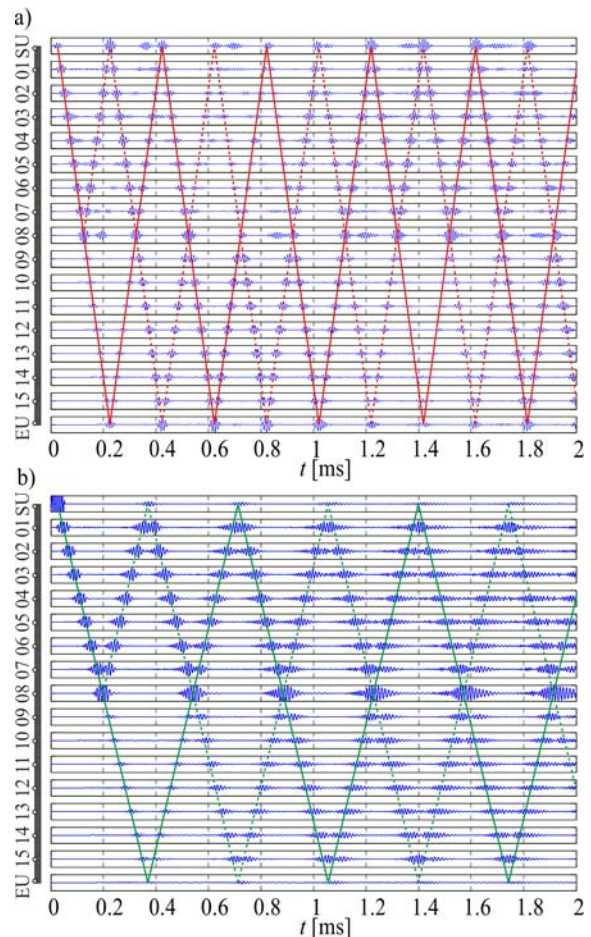


Fig. 13. Numerical signals for sample B: a) scheme L, axial acceleration, b) scheme F, transverse acceleration

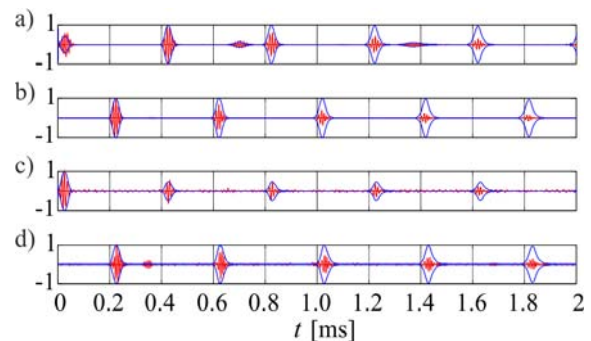


Fig. 14. Comparison of numerical and experimental signals of sample A: a) scheme L, point 1, b) scheme L, point 2, c) scheme F, point 1, d) scheme F, point 2

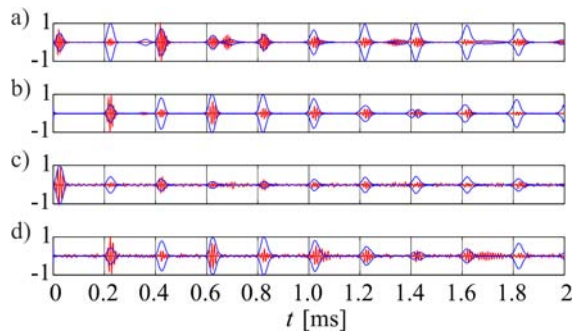


Fig. 15. Comparison of numerical and experimental signals of sample B: a) scheme L, point 1, b) scheme L, point 2, c) scheme F, point 1, d) scheme F, point 2

## 5.2. Single lap adhesive joints

A significant question for single lap adhesive joints may be determination of the overlap length. It is possible based on acceleration maps and signals of wave propagation in the points at the ends of the sample. Figure 16 presents the history of propagation of S0 mode in specimen C4. At the start (Fig. 16a) wave W0 hit the end of the overlap and is divided into three parts: W1 that propagates in the same direction as primary wave, W2 that is reflected in the lower rod and W3 that is also reflected but propagates in the upper rod. Later (Fig. 16b) both W2 and W3 meet at the other end of the overlap. Part W2 propagates further in the lower rod but W3 is reflected as W4 and W5 propagating in the upper and lower rods, respectively. In the next time instance (Fig. 16c) wave W4 propagates in upper rod whereas part W5 is reflected at the end of the overlap. In the end waves W1 and W4 reaches one end of the sample (Figs. 16d and 16f) whereas W2 and W5 arrives to another end (Figs. 16e and 16g). The time interval between arrivals of adequate parts is the time of double passing through the joint overlap.

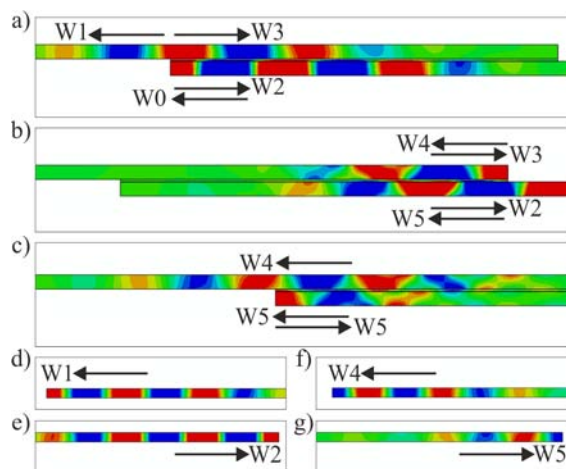


Fig. 16. History of S0 mode propagation (sample C4, scheme L) for particular time instances: a) 0.0136 ms, b) 0.0180 ms, c) 0.0212 ms, d) 0.0240 ms, e) 0.0248 ms, f) 0.0288 ms, g) 0.0332 ms

Figure 17 shows normalized signals collected at the end point (E) of the samples C1-C4 in scheme L. The objects of interest are the first two wave packets. Knowing the group velocity of S0 mode (determined before) and the time interval between these two packets, it is possible to calculate the overlap length. The results for specimens C1-C4 are: 43.5 mm, 84.8 mm, 123.2 mm and 165.4 mm, respectively. Received values are compatible with the real overlap length implemented in the models.

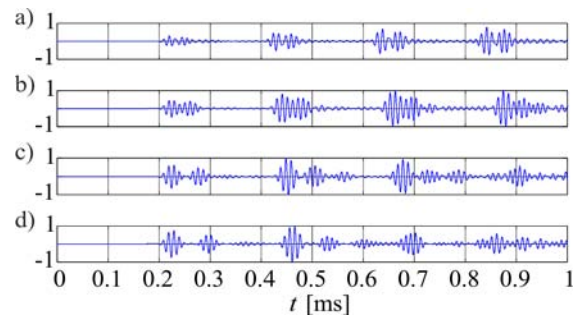


Fig. 17. Signals of propagated wave collected at E point for single lap joints (scheme L): a) C1, b) C2, c) C3, d) C4

The comparison of experimental and numerical results for specimen C1 do not go as well as for samples A and B. Signals are more difficult for interpretation because when the wave passes through the lap joint, a mode conversion may occur. At the edge of the overlap the wave is transmitted from a single-layer medium to a three-layer one. The results are vulnerable to inaccuracies in geometry and material properties. A good agreement is observed only at the beginning of the signals, before passing through the joint. Further signals differ significantly.

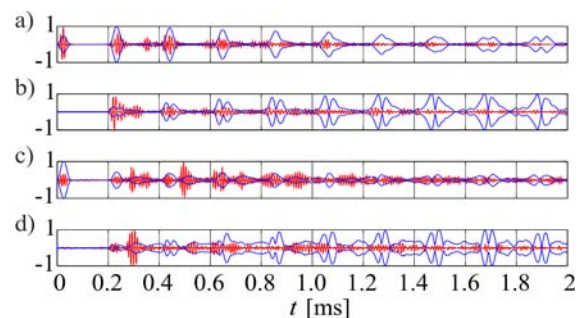


Fig. 18. Comparison of numerical and experimental signals of sample C1: a) scheme L, point 1, b) scheme L, point 2, c) scheme F, point 1, d) scheme F, point 2

## 6. CONCLUSIONS

The paper relates to the problem of adhesive joints of metal members. The results of research carried on glue connections of metal rods were discussed. Numerical and experimental approach was applied. Guided wave propagation in the butt joint associated with simultaneous partial reflection

and transmission of symmetrical and antisymmetric modes through the adhesive layer. Based on recorded signals, determination of the joint existence was possible. For the single lap joint, mode conversion phenomenon and multimodal character of propagation was observed. In specimens with varied length of overlay, the overlap length was identified based on wave propagation signals.

Techniques based on guided wave propagation found large opportunities for non-destructive diagnostics of engineering structures. Executed analyses are the first step for further research dealing with non-destructive testing of structural adhesive joints of metal elements.

### ACKNOWLEDGEMENTS

The research work was carried out within the project No. 2015/19/B/ST8/00779, financed by the National Science Centre, Poland.

Calculations were carried out at the Academic Computer Centre in Gdańsk.

### REFERENCES

- Adams RD, Wake WC. *Structural Adhesive Joints in Engineering*. 1st ed. London and New York: Elsevier Applied Science Publishers; 1984. DOI:10.1007/978-94-009-5616-2.
- Barski M, Kędziora P, Muc A. Structural Health Monitoring (SHM) Methods in Machine Design and Operation. *Archive of Mechanical Engineering* 2014; LXI: 653-677. DOI: 10.2478/meceng-2014-0037
- Bocchini P, Marzani A, Viola E. Graphical User Interface for Guided Acoustic Waves. *Journal of Computing in Civil Engineering* 2010; 25(3): 202-210. DOI: 10.1061/(ASCE)CP.1943-5487.0000081
- Dillard DA. *Advances in Structural Adhesive Bonding*. 1st ed. Oxford, Cambridge, New Delhi: Woodhead Publishing Limited; 2010.
- Hagl A. How to Join Steel and Glass: Complex Adhesive Behaviour. *Eurosteel* 2008; 929-946.
- Kędra R, Rucka M. Diagnostics of bolted lap joint using guided wave propagation. *Diagnostyka* 2014; 15(4): 35-40.
- Korzeniowski M, Piwowarczyk T, Maev RG. Application of ultrasonic method for quality evaluation of adhesive layers. *Archives of Civil and Mechanical Engineering* 2014; 14: 661-670. <https://doi.org/10.1016/j.acme.2013.10.013>
- Lanza di Scalea F, Bonomo M, Tuzzeo D. Ultrasonic Guided Wave Inspection of Bonded Lap Joints: Noncontact Method and Photoelastic Visualization. *Research in Nondestructive Evaluation* 2001; 13: 153-171. DOI: 10.1007/s00164-001-0016-8
- Łagoda M. *Strengthening of bridges by elements' gluing*. Kraków: Wydawnictwo Politechniki Krakowskiej; 2005. Polish.
- Meinz J. *Kleben im Stahlbau, Betrachtungen zum Trag- und Verformungsverhalten und zum Nachweis geklebter Trapezprofilanschlüsse und verstärkter Hohlprofile in Pfosten-Riegel-Fassaden*. Berlin: Weißensee Verlag; 2010.
- Moser F, Jacobs LJ, Qu J. Modelling elastic wave propagation in waveguides with the finite element method. *Nondestructive Testing and Evaluation International* 1999; 32: 225-234. DOI: 10.1016/S0963-8695(98)00045-0
- Piekarczyk M, Grec R. Application of adhesive bonding in steel and aluminium structures. *Archives of Civil Engineering* 2012; LVIII(3): 309-329. DOI: 10.2478/v.10169-012-0018-8
- Rokhlin SI. Lamb wave interaction with lap-shear adhesive joints: Theory and experiment. *The Journal of the Acoustical Society of America* 1991; vol. 89: 2758-2765. DOI: 10.1121/1.400715
- Rucka M. *Guided wave propagation in structures, Modelling, experimental studies and application to damage detection*. Gdańsk: Wydawnictwo Politechniki Gdańskiej; 2011.
- Zima B, Rucka M. Non-destructive inspection of ground anchors using guided wave propagation. *International Journal of Rock Mechanics & Mining Sciences* 2017; 94: 90-102. <https://doi.org/10.1016/j.ijrmmms.2017.03.005>

Received 2017-09-24

Accepted 2017-11-03

Available online 2017-11-06



**Erwin WOJTCZAK**, M.Sc. is an assistant at the Department of Mechanics of Materials and Structures, Gdansk University of Technology. He graduated civil engineering at the Faculty of Civil and Environmental Engineering. Since October 2017 he continues his education as a Ph.D. student. He mainly deals with non-destructive diagnostics of adhesive joints.



**Magdalena RUCKA**, Ph.D., D.Sc. is an associate professor at the Department of Mechanics of Materials and Structures, Gdansk University of Technology. Her scientific interests are focused on the dynamics of structures, wave propagation and development of new techniques for damage detection and structural health monitoring.